A depth-dose measuring device using a multichannel scintillating fiber array for electron beam therapy

Takahiko Aoyama, Shuji Koyama, Masatoshi Tsuzaka, and Hisashi Maekoshi
Nagoya University College of Medical Technology, Daikominami, Higashi-ku, Nagoya 461, Japan

(Received 13 September 1996; accepted for publication 6 May 1997)

The development of a new depth-dose measuring device for electron beam therapy is described. The device employs plastic scintillating fiber detectors inserted in a polymethylmethacrylate (PMMA) phantom in line along an incident electron beam. Output photons from a fiber, the number of which is proportional to the absorbed dose at each depth of the phantom, were converted to an electric signal with a photodiode. Each signal from the photodiode was transmitted to a personal computer through a multichannel analog–digital converter, and was processed to draw a depth-dose curve on the computer display. A depth-dose curve could be obtained in a measuring time of 5 s for each incident electron beam with an energy range between 4 and 21 MeV. The mean electron energies estimated using the curves and the depth-scaling factor for PMMA were consistent with those obtained from conventional depth-dose measurements using an ion chamber and a water phantom. The newly developed system, being simple and not time consuming, could be used routinely for quality assurance purposes in electron beam therapy. © *1997 American Association of Physicists in Medicine.* [S0094-2405(97)02308-0]

Key words: electron beam, depth-dose measurement, beam energy, quality assurance, scintillating fiber

I. INTRODUCTION

Electron beam therapy requires the information of absorbed dose distributions in tissue for the exact beam to be used. Measurements of depth-dose curves have been carried out using a small volume ion chamber placed at various depths in a tissue-equivalent material, where water was used as a standard material. Since the construction of the ion chamber is different from that of the surrounding material, complicated correction is required to convert ion chamber readings to absorbed doses. In recent years, a miniature water-equivalent plastic scintillator with an optical fiber light guide was used for measuring depth-dose curves.[1,2] Since light output from the scintillator is proportional to the absorbed dose in water, no correction is needed in this case.

The present paper describes a convenient method that can directly measure absorbed dose distributions in a tissue-equivalent material in a short time. The method uses plastic scintillating fibers inserted in a plastic phantom in line along an incident electron beam. For a single irradiation of an electron beam, an output signal, the intensity of which is proportional to the absorbed dose at each depth of the phantom, was obtained simultaneously from each fiber, and was processed with a personal computer to draw a depth-dose curve on the computer display.

II. DESCRIPTION OF THE DEVICE

A. Scintillating fiber detector

Figure 1 shows the construction of the detector part of the depth-dose measuring device. The part consists of 12 scintillating fibers, of 1 mm diam, which were inserted into a $32 \times 32 \times 10\ \mathrm{cm}^3$ polymethylmethacrylate (PMMA) phantom in line along the central axis of an electron beam with a constant spacing of 8 mm. A phantom thickness of 10 cm was selected for measuring electron beams with incident electron energy of less than 25 MeV. Light emitted from each fiber on the exposure of the phantom to an electron beam was detected with a photodiode connected at an end of the fiber.

High-energy electrons that entered the fibers generate Čerenkov radiation in addition to scintillation light. Since Čerenkov radiation is not directly proportional to the dose delivered in the fibers, it results in background when detected with the photodiodes. The background due to Čerenkov radiation is known as the ''stem effect'' for a scintillator dosimeter[1] consisting of a miniature plastic scintillator with an optical fiber light guide, where the Čerenkov component can be subtracted by using light signal from a twin fiber without scintillator. It was found that the maximum Čerenkov contribution occurred at the depth of the shoulder of a depth-dose curve,[3] where it amounted to 12%[1] when used with a scintillator that was 4 mm long, 1 mm in diameter, with an optical fiber light guide, and placed at the center of a $10 \times 10\ \mathrm{cm}^2$ irradiation field. In our case, using long scintillating fibers, since scintillation contribution is 13 times larger for the same field size, the background Čerenkov contribution would be reduced to the order of 1% at maximum. Considering the accuracy of our depth-dose measurements it is concluded that the Čerenkov contribution can be completely neglected.

The scintillating fibers used are styrene-based Bicron BCF-60 with an emission peak of 530 nm (green)—the fibers emit photons of ~7100/MeV for a minimum ionizing particle. Since electron mass stopping powers by collision for polystyrene are only 0.3%–0.6% larger[4] than those for

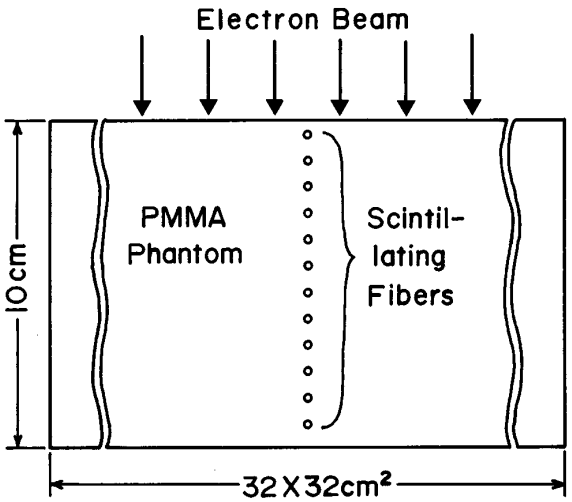

FIG. 1. Construction of the detector part of the depth-dose measuring device.

PMMA for an electron energy range from 20 to 0.2 MeV, at which energy the range of electrons is less than the radius of the fiber, no correction would be needed to estimate absorbed doses in PMMA from scintillating fiber readings.

Figure 2 shows the details of the connection between scintillating fibers and photodiodes. Centering of a fiber and a cylindrical photodiode was carried out using a coaxial brass sleeve. For the external light shield, colloidal graphite was applied to each fiber and the outside of the PMMA phantom. A copper plate, 10 mm thick, was placed above the photodiode array to cut off the effect by electron beam leakage, since the direct hit of a high-energy electron on a photodiode produces about 100 times larger output in the photodiode.

B. Electronics

Output light from scintillating fibers could be detected with unity-gain photodiodes without using photomultipliers, since it was strong enough for dose rates of several Gy/min from therapeutic accelerators. The photodiodes used are Hamamatsu S1336-18BK with a sensitive area of 1.1×1.1 mm^2. Quantum efficiency of the photodiode was estimated to be 66% for 530 nm photons emitted from the BCF-60 fibers.

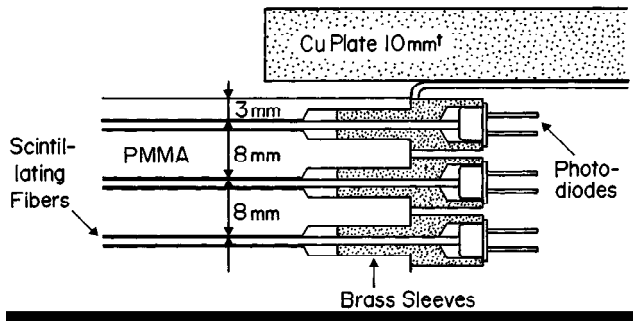

FIG. 2. Details of the detector showing the connection between a scintillating fiber and a photodiode.

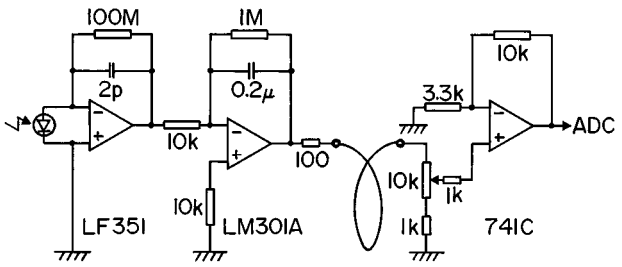

FIG. 3. The amplifier circuit for the photodiode; resistor in Ω, and capacitor in F.

Figure 3 shows an amplifier circuit for the photodiodes. The basic design of the circuit is the same as that used for a scintillating fiber beam-energy monitor.[5] Electron beams from therapeutic accelerators consist of a train of pulses, for instance with a width of a few μs distributing at about 10 ms intervals for the linear accelerators used. To obtain a large signal-to-noise ratio with simple electronics, pulse charges induced in each photodiode were converted into a voltage pulse proportional to the number of photons emitted using a charge-sensitive preamplifier, and then integrated into a dc voltage. dc voltages derived from each channel of 12 scintillating fibers were fed through a multiwire cable of 15 m to a buffer amplifier with variable gain placed in an accelerator control room, and then to a 16-channel analog-to-digital converter (ADC). Digital voltages from each channel were processed with a personal computer to draw a depth-dose curve on the computer display.

III. SENSITIVITY CORRECTION FOR EACH FIBER CHANNEL

Uniform sensitivity of each channel is the key when used with a multichannel scintillating fiber array detector to measure dose distributions. The sensitivity defined as an output voltage for a given number of photons emitted in a scintillating fiber would be affected by various factors such as light transmission in the fiber, nonoptimized optical coupling between the fiber and the photodiode, and electronic gain at each stage of the amplifiers.

The sensitivity of each channel could be measured accurately using the exponential attenuation characteristic of x-ray beam intensity in matter. It is well known that when a narrow x-ray beam is irradiated in a tissue equivalent material the absorbed dose increases with depth at first and then decreases exponentially with increasing depth. To use the latter exponentially decreasing portion of depth-dose curves, x-ray beams were irradiated on the scintillating fiber array detector through an additional PMMA plate with a thickness of more than the maximum range of secondary electrons. For 10 MV x rays used in our experiment, the addition of a 5-cm-thick PMMA plate was enough, since the continuous slowing down approximation range of 10 MeV electrons was estimated to be about 4.3 cm in the same medium.[4]

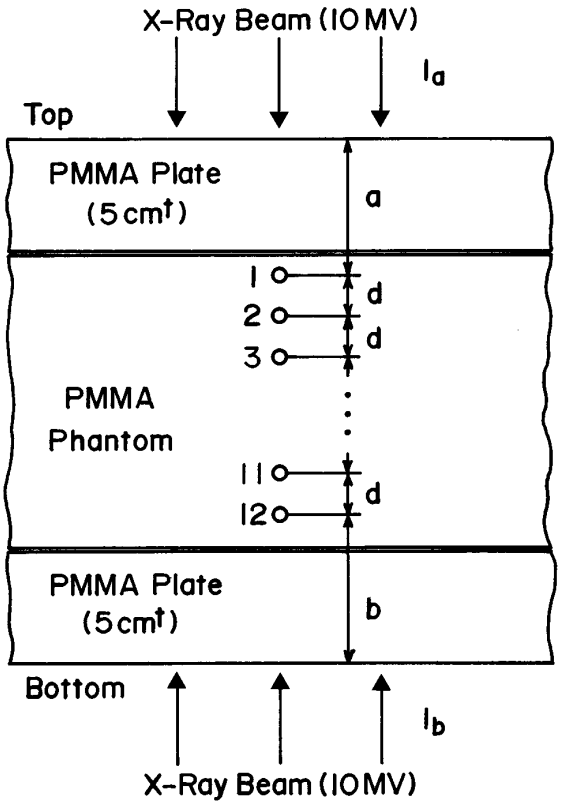

FIG. 4. Schema of the sensitivity measurement.

Figure 4 shows the schema of sensitivity measurement. When a 10 MV x-ray beam with an intensity of I_a is irradiated through a thick PMMA plate on the top of the phantom, the output voltage V_{tj} at the jth fiber position is expressed with a sensitivity f_j of the form

$$V_{tj}=I_a\cdot\exp[-\mu\{a+(j-l)d\}]\cdot K\cdot f_j, \tag{1}$$

where μ is the effective x-ray attenuation coefficient, a the depth of the first scintillating fiber, d the interval between adjacent fibers in the PMMA phantom, and K is the conversion factor from x-ray intensity to the number of photons emitted in the fiber. Reversing the incident direction of the x-ray beam from top to bottom, the output voltage V_{bj} at the same jth fiber position is expressed in the form

$$V_{bj}=I_b\cdot\exp[-\mu\{b+(12-j)d\}]\cdot K\cdot f_j, \tag{2}$$

where I_b is the intensity of the x-ray beam, and b is the depth of the 12th fiber from the surface of the additional PMMA plate. Multiplying V_{bj} by V_{tj} we obtain the quantity proportional to f_j^2 alone for each fiber position:

$$V_{tj}\cdot V_{bj}=I_a\cdot I_b\cdot\exp[-\mu(a+b+11d)]\cdot K^2\cdot f_j^2$$
$$=\text{const}\cdot f_j^2. \tag{3}$$

Figure 5 shows relative output voltages at each fiber position observed from x-ray beam irradiation from the top and the bottom directions. An irradiation field of $10\times 10\ \text{cm}^2$ was used in the measurements. Sensitivity at each fiber position or channel was calculated substituting the data in Fig. 5 into Eq. (3), and it was used to correct output voltages of each channel. Figure 5 also shows the relative output voltages corrected for the raw data obtained from x-ray beam irradiation from the top direction and an exponential fitting curve for the corrected data. Excellent agreement for the fitting curve within an error of $\pm 0.3\%$ indicates the validity of the exponential decrease of x-ray dose with increasing depth in the medium.

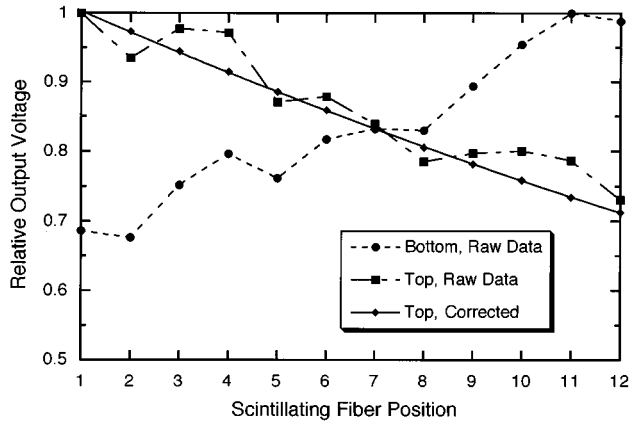

FIG. 5. Relative output voltages at each fiber position observed from x-ray beam irradiation from the top and bottom directions. Also shown are the relative output voltages corrected for the raw data obtained from x-ray beam irradiation from the top direction and an exponential fitting curve for the corrected data.

IV. DEPTH-DOSE MEASUREMENT FOR ELECTRON BEAMS

The output voltage derived from each channel of the detector and corrected for its sensitivity is proportional to the linear integral of absorbed dose with respect to fiber length. If the mean energy and the mean incident direction of an electron beam are uniform in an irradiation field, the distribution of the absorbed dose integral obtained from our measurement would be consistent with the depth-dose curve in PMMA measured along the central axis of the electron beam. In actual cases, the mean energy and the mean incident direction of an electron beam are not completely uniform in the irradiation field, and they depend on the type of applicator or collimator used. The difference of the mean electron energy—and of the mean incident direction also—was estimated from Monte Carlo simulation[6] and it was found to be within a few percent—e.g., 0.4 MeV for an 18 MeV beam from a Clinac 2100C accelerator, $10\times 10\ \text{cm}^2$ field—over an irradiation field at phantom surface, where the difference becomes maximum, using typical applicators. Since electron mass stopping powers by collision are nearly constant for an electron energy range of 5–25 MeV with a slowly increasing rate of less than 1% per MeV in polystyrene,[4] they can be considered to be constant along the fiber axis over an irradiation field. Considering that the absorbed dose is proportional to mass stopping power by collision, the discrepancy between depth-dose integral curves and depth-dose curves can be neglected for typical irradia-

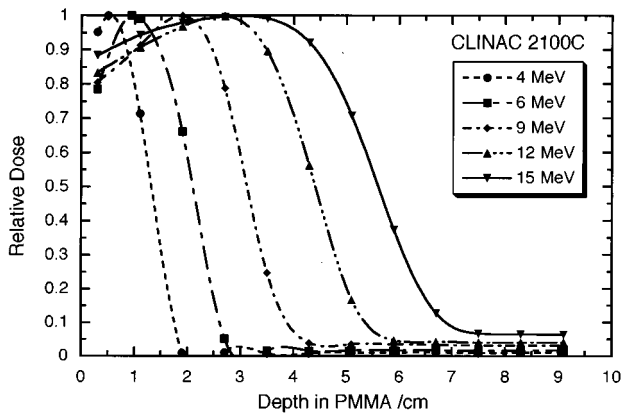

FIG. 6. Relative doses as a function of depth in PMMA observed for the Clinac 2100C accelerator for various energies of electron beams (energies are nominal). The markers shown are measured points except for the maximum dose for 4 and 6 MeV beams. Curves were drawn using spline interpolation, where the maximum dose was normalized to unity for each curve.

tion conditions. In this paper, depth-dose integral curves obtained from our measurements will be simply referred to as depth-dose curves.

Dose distributions observed for various energies of electron beams are shown in Figs. 6 and 7 as a function of depth in PMMA, where Fig. 6 was obtained for Clinac 2100C and Fig. 7 for Mevatron KD77 linear accelerators. Irradiation field size was 10×10 cm^2 at the phantom surface using appropriate applicators for the usual source-to-surface distance of 100 cm. For each beam energy, 100 sampling voltages were taken into the computer memory in a measuring time of 5 s through the 16-channel ADC, and the ratio of the voltage at each channel to that at the first channel was averaged on the computer over 100 sampling points. After sensitivity correction was carried out for each channel, depth-dose curves were drawn using spline interpolation—the curves which are shown in Figs. 6 and 7—where the maximum dose was normalized to unity for each curve. It should be noticed that the curve for the 4 MeV beam from the Clinac 2100C was drawn using only three measured points and hence it merely gives an outline of the dose distribution.

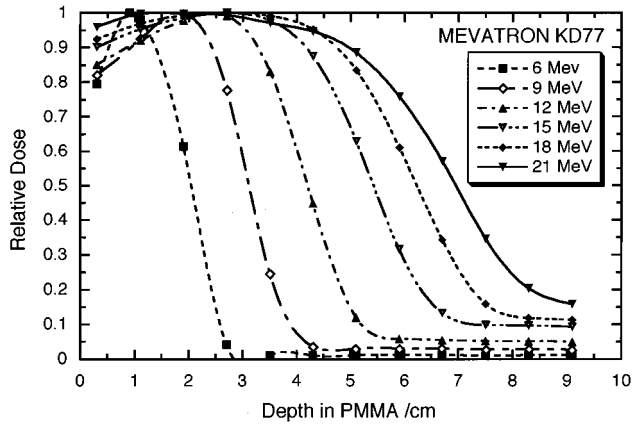

FIG. 7. Relative doses as a function of depth in PMMA observed for the Mevatron KD77 accelerator for various energies of electron beams (energies are nominal). The markers shown are measured points except for the maximum dose for the 6 MeV beam. Curves were drawn using spline interpolation, where the maximum dose was normalized to unity for each curve.

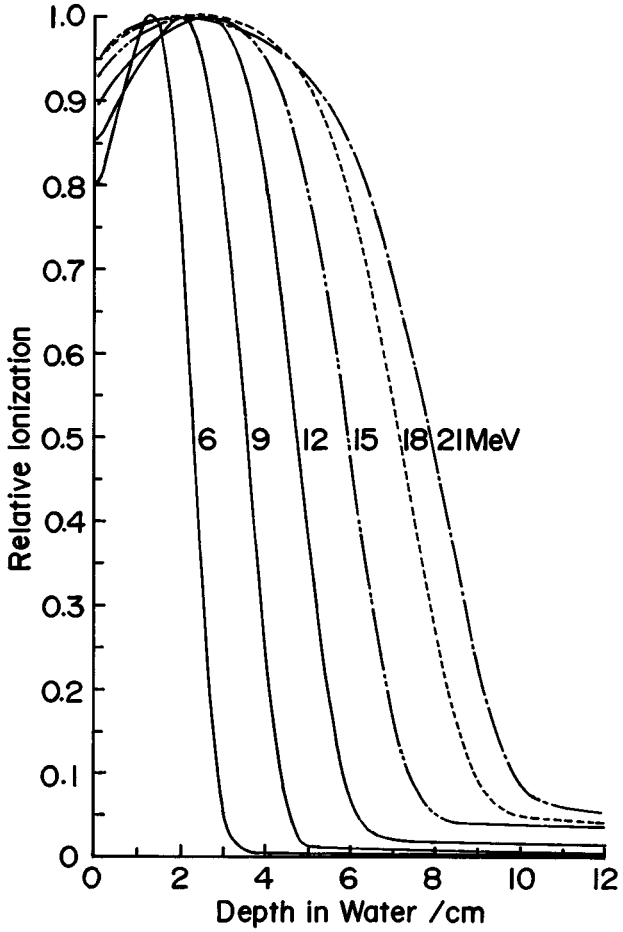

FIG. 8. Depth-ionization curves measured for the Mevatron KD77 accelerator by the standard method using an ion chamber and a water phantom, 10×10 cm^2 field.

The shape of each curve seen in Figs. 6 and 7 was approximately consistent with that of the corresponding depth-ionization curve measured by the standard method using an ion chamber and a water phantom, except for a relatively high background level where depth-ionization curves for Mevatron KD77 are shown in Fig. 8. The two or three times larger background components seen in Figs. 6 and 7 at the depths larger than the maximum ranges of incident electrons might be due to a large irradiation field for bremsstrahlung x rays generated in the scattering foil of the accelerator, and in the applicator and the phantom, where the x rays would be detected in the whole length of scintillating fibers.

The mean energy E_0 of an electron beam at the surface of a phantom can be estimated from a depth-dose curve using the depth d_{50} of 50% dose level in water:

$$E_0 = 2.33 \times d_{50} \ [\text{MeV}], \tag{4}$$

where the depth d_{50} is given in cm, and the value of 2.33

TABLE I. The depth of 50% dose level in PMMA, d'_{50}, and the mean energy of an electron beam, E_0, estimated using the data of Figs. 6 and 7 at each beam energy. The values in parentheses are the mean energies obtained from conventional depth-dose measurements using an ion chamber and a water phantom.

Electron beam energy (in nominal) [MeV]	Clinac 2100C		Mevatron KD77	
	d'_{50} [cm]	E_0 [MeV]	d'_{50} [cm]	E_0 [MeV]
6	2.12	5.6 (5.6)	2.04	5.4 (5.4)
9	3.12	8.2 (8.3)	3.12	8.2 (8.4)
12	4.40	11.6 (11.4)	4.20	11.1 (11.2)
15	5.60	14.8 (14.7)	5.44	14.4 (14.2)
18			6.24	16.5 (17.1)
21			6.96	18.4 (18.8)

MeV/cm was recommended by the AAPM TG-21 protocol as an average in the electron-beam-energy range of 5–50 MeV.

It is well known that the depth-dose curve measured in other tissue-equivalent material than water was consistent with that in water if the depth-scaling factor ρ_{eff} was multiplied by the depth of the material. The factor $\rho_{\text{eff}} = 1.132$ was found for PMMA from Monte Carlo calculations[6] and experiments.[7] Using the depth d'_{50} of 50% dose level in PMMA and the depth-scaling factor ρ_{eff} the depth d_{50} in water is then given in the form

$$d_{50} = d'_{50} \times \rho_{\text{eff}}. \tag{5}$$

The mean electron beam energies E_0 were calculated by substituting the values of d'_{50} obtained from Figs. 6 and 7 into Eqs. (4) and (5). The results are shown in Table I with the values of d'_{50}. Also shown in Table I are values of E_0 (in parentheses) obtained from the standard depth-dose measurements using an ion chamber and a water phantom. The values of E_0 for 18 and 21 MeV beams were a few percent smaller than those from the standard method because the irradiation field is not large enough compared with the values of d'_{50}. The consistency of the values of E_0 for 6–15 MeV beams indicates that our method can also be used to check electron beam energy.

V. CONCLUSIONS

The newly developed depth-dose measuring device using a multichannel scintillating fiber array detector with a computer data-readout system has several advantages over conventional ion-chamber-based devices.

(1) The use of minimally disturbing plastic scintillating fibers inserted in a plastic phantom creates an ideal dose measuring system for electron beams.
(2) The intensity of the output signal from scintillating fibers is proportional to the absorbed dose in the fibers. Using the fibers with the same collision stopping powers as those of the phantom, complicated correction required for the ion chamber measurements is unnecessary to estimate dose distributions in the phantom.
(3) The fluctuation of electron beam intensity in a measuring time has no effect on observed data because of simultaneous data acquisition from each channel of the scintillating fiber array detector.
(4) The use of a multichannel ADC and a personal computer data acquisition system allows us to obtain depth-dose data automatically in a short time of 5 s.
(5) Mean electron beam energy calculated on the computer from depth-dose data can be used to check the constancy of electron beam energy.

The number of scintillating fiber channels in the phantom was not large enough, which resulted in medium accuracy for depth-dose measurements. The newly developed system, however, being simple and not time consuming for the measurements, would be used routinely for quality assurance purposes for electron beam therapy.

ACKNOWLEDGMENTS

The authors would like to thank Satoru Kondo, Yuichi Aoyama, Shinji Abe, and Mitsuhiko Homma of Nagoya University Hospital for their helpful support of the irradiation of electron and x-ray beams from clinical accelerators.

[1] A. S. Beddar, T. R. Mackie, and F. H. Attix, ''Water-equivalent plastic scintillation detectors for high-energy beam dosimetry,'' Phys. Med. Biol. **37**, 1883–1913 (1992).
[2] D. Flühs, M. Heintz, F. Indenkämpen, C. Wieczorek, H. Kolanoski, and U. Quast, ''Direct reading measurement of absorbed dose with plastic scintillators—The general concept and applications to ophthalmic plaque dosimetry,'' Med. Phys. **23**, 427–434 (1996).
[3] A. S. Beddar, T. R. Mackie, and F. H. Attix, ''Cerenkov light generated in optical fibres and other light pipes irradiated by electron beams,'' Phys. Med. Biol. **37**, 925–935 (1992).
[4] F. H. Attix, *Introduction to Radiological Physics and Radiation Dosimetry* (Wiley, New York, 1986).
[5] T. Aoyama, H. Maekoshi, M. Tsuzaka, and S. Koyama, ''A scintillating fiber beam-energy monitor for electron beam therapy,'' Med. Phys. **22**, 2101–2102 (1995).
[6] G. X. Ding, D. W. O. Rogers, and T. R. Mackie, ''Mean energy, energy-range relationships and depth-scaling factors for clinical electron beams,'' Med. Phys. **23**, 361–376 (1996).
[7] M. S. Huq, A. G. Agostinelli, and R. Nath, ''An evaluation of the recommendations of the TG-25 protocol for determination of depth dose curves for electron beams using ionization chambers,'' Med. Phys. **22**, 1333–1337 (1995).